Subsurface Sensing Technologies and Applications Vol. 2, No. 3, July 2001 (©2001)

Modeling Clutter from Bosnian and Puerto Rican Rough Ground Surfaces for GPR Subsurface Sensing Applications Using the SDFMM

Magda El-Shenawee

Department of Electrical Engineering, 3217 Bell Engineering Center, University of Arkansas, Fayetteville, AR 72701

Carey M. Rappaport

Center for Subsurface Sensing and Imaging Systems, Department of Electrical and Computer Engineering, Northeastern University, 235 Forsyth BLD, Boston, MA 02115

Received January 25, 2001; Revised April 7, 2001

The Steepest Descent Fast Multipole Method (SDFMM) is used to analyze the distorting effect of random rough ground surfaces on scattered and transmitted electromagnetic waves. Two well-measured loamy soils: Bosnian and Puerto Rican clay loam are investigated, each with a variety of surface roughness. This study is important in understanding the effects of different soil properties and is meant to be an *a priori* phase of investigating scattering from buried targets under the rough ground. In this work, we investigated the scattering from rough soil ground without buried objects. The SDFMM is an integral equation-based fast algorithm that is well suited for two-dimensional penetrable rough surfaces (3-D scattering) in the frequency domain. The scattered and transmitted near electric field of an incident Gaussian beam are calculated at different locations above and below the mean plane of the dielectric rough interface. The receiver locations above are chosen to simulate GPR measurement protocols. The obtained numerical results show that the scattered field undergoes more distortion than the transmitted field from both soil types. Moreover, the transmitted fields into the higher dielectric constant Puerto Rican soil experience more distortion than those transmitted into Bosnian soil.

Key Words. Rough surface scattering, GPR, EM modeling, fast algorithms.

1. Introduction

When electromagnetic waves are used to sense buried objects, the effect of the random rough air/ground interface on both the transmitted

1566-0184/01/0700-0249$19.50/0

and scattered fields is great, and must be carefully considered. In many cases, the scattering from the air/ground interface is larger than the scattering of a buried target especially when the ground surface roughness is comparable to the height and the burial depth of the target. Accurate modeling of the clutter is necessary to enable signal-processing algorithms to perform optimally in detecting buried targets. In this work, we investigate the clutter of different types of soil, which is scattering from rough surface without any buried targets.

The rough surface causes two types of distorting effects on a probing plane wave: a defocused scattered wave reflected back into the air, and a distorted transmitted wave that would continue until it encounters a target. Uncertainty is generated in both waves, and it is important to understand the relative amounts of distortion between the two, as well as its dependence on soil type. While there has been much published work on far field rough surface scattering [1–8], the near field effects—which are essential in inverse scattering and object sensing applications—have not been well studied. However, there is published work for modeling near field from targets buried under planar surface [9]. As an effort to study the scattered fields in the near zone, we assumed that the incident waves are still far fields while point receivers are located in the near zone above and below the rough ground. No interactions between scattered fields and the transmitting antenna are accounted for in this work.

The surface scattering depends on the frequency dependent complex dielectric constant of the soil, which in turn depends on its composition, moisture and density, and also on the roughness of the surface. As moisture increases, so does the dielectric constant. And with a larger dielectric constant, the wavelength in soil decreases. For a given illuminated portion of ground, wetter soil will require finer computational discretization, and greater computational expense. However, using special-purpose numerical methods, the fast computation of wave interaction with a rough surface is feasible. We study two types of experimentally measured soil: Bosnian loam from the Alicia test site [10], and Puerto Rican clay loam [11].

The rough surface is characterized with Gaussian statistics in terms of random heights and autocorrelation function [12]. The roughness parameters (root mean square height and correlation length) are chosen to be in the moderate roughness range, with root mean square height ranging from 0.1 to 0.2 free space wavelengths and the correlation length kept constant at one free space wavelength.

In this work, a specialized fast algorithm is necessary, since multiple calculations of this realistic, but computationally intensive, model are needed for many different realizations of surface roughness. Therefore we used the SDFMM, which is a hybridization of the Method of Moments

(MOM), the Steepest Descent Path (SDP) method, and the Fast Multipole Method (FMM) [13,14], to calculate the unknown surface current coefficients. The details of the SDFMM can be found in [15–18].

2. Formulation

In this work, the well-known PMCHW (Poggio, Miller, Chang, Harrington, and Wu) integral equations are implemented to calculate the electric and magnetic surface currents [16,19]. For convenience, the integral equation are summarized here as

$$\bar{E}^{\text{inc}}(\bar{r})\big|_{\tan} = [(L_1 + L_2)\bar{J}_1 - (K_1 + K_2)\bar{M}_1]_{\tan} \tag{1}$$

and

$$\bar{H}^{\text{inc}}(\bar{r})\big|_{\tan} = \left[(K_1 + K_2)\bar{J}_1 + \left(\frac{L_1}{\eta_1^2} + \frac{L_2}{\eta_2^2}\right)\bar{M}_1\right]_{\tan} \tag{2}$$

in which $\bar{E}^{\text{inc}}(\bar{r})$ and $\bar{H}^{\text{inc}}(\bar{r})$ are the incident electric and magnetic fields on the interface between air and soil as shown in Figure 1. The subscript tan

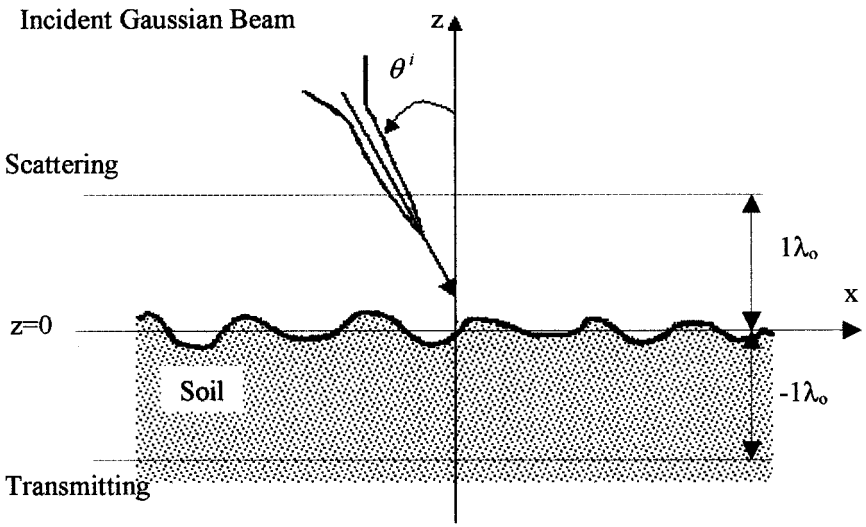

Figure 1. Cross section of rough soil ground with Gaussian beam incident at θ^i.

means the tangential component. The differentio-integral operators L_1, L_2, K_1 and K_2 are defined as [19]

$$L_{1,2}\bar{X} = \int_S \left\{ i\omega\mu_{1,2}\Phi_{1,2}\bar{X}(\bar{r}') + \frac{i}{\omega\varepsilon_{1,2}}\nabla\nabla'\cdot\bar{X}(\bar{r}')\Phi_{1,2} \right\} ds' \tag{3a}$$

$$K_{1,2}\bar{X} = \int_S \bar{X}(\bar{r}')\times\nabla\Phi_{1,2}\, ds' \tag{3b}$$

where the vector $\bar{X}$ represents the surface electric current $\bar{J}$ or the surface magnetic current $\bar{M}$ on the interface S. The dielectric permittivity and permeability in each region are ε_i and μ_i, $i = 1$ and 2. The 3-D scalar Green's function in $\Phi_i(\bar{r})$ is given by

$$\Phi_i(|\bar{r}-\bar{r}'|) = \frac{\exp(-ik_i|\bar{r}-\bar{r}'|)}{4\pi|\bar{r}-\bar{r}'|} \tag{3c}$$

in which $\bar{r}$ is the field point, $\bar{r}'$ is the source point, $k_i = \omega\sqrt{\varepsilon_i\mu_i}$ is the wave number in each region, $i = 1$ and 2. The equivalent electric and magnetic currents $\bar{J}$ and $\bar{M}$ on S, are approximated using the RWG vector basis functions $\bar{j}(\bar{r})$ [19,20] as follows

$$\bar{J}(\bar{r}) = \sum_{n=1}^{N} I_{1n}\bar{j}_n(\bar{r}), \qquad \bar{r}\in S \tag{4a}$$

$$\bar{M}(\bar{r}) = \eta_1 \sum_{n=1}^{N} I_{2n}\bar{j}_n(\bar{r}), \qquad \bar{r}\in S \tag{4b}$$

where η_1 is the intrinsic impedance of the free space. Upon substituting Eq. (3–4) in Eqs. (1) and (2) and testing with the same basis functions, we get the $2N\times 2N$ system of equations as

$$\bar{\bar{Z}}\bar{I} = \bar{V} \tag{5}$$

in which $\bar{V}$ represents the tangential component of the electric and magnetic fields, $\bar{I}$ represents the unknown coefficients, and $\bar{\bar{Z}}$ is the impedance matrix [19]. Solving Eq. (5) using the method of moments is extremely expensive (computer memory and CPU time) when the size of the scatterer (the rough interface, in this case) is much larger than the free space wavelength. In reality, the size of the ground is infinite but for computational consideration the rough ground is assumed to be adequately larger than the footprint of the incident Gaussian beam [21]. As the number of unknown coefficients is very large, special computational procedures must be used such as the SDFMM, which is discussed in [15–18] and recently was implemented in [22].

3. Numerical Results

We consider the scatterer S to be a penetrable random rough surface with dimensions equal to $L \times L$, where $L = 8\lambda_0$, and λ_0 is the free space wavelength. Exciting the surface with a carefully tapered incident Gaussian beam minimizes the edge effect of the surface S on the surface currents [21]. Thus, infinitely large rough surfaces are sampled over a manageable region. The random rough surface is characterized with Gaussian statistics for the random heights and for the autocorrelation function, and is generated using the computer random number generator following the technique in [12]. Sixty Monte Carlo rough surface simulations were calculated for each pair of Gaussian parameters: root mean square height σ and correlation length l_c. For cases considered here, the electric field is assumed to be x-directed, and normally incident ($\theta^i = 0$) on the nominal ground surface.

Similar to the work in [16], which implemented the SDFMM to calculate the radar cross section of a penetrable random rough surface, we also are using the SDFMM but to calculate the near electromagnetic fields scattered above and transmitted into the ground.

Point receivers are located in the near zone at one wavelength above and below the mean ground with resolution equal to $x = y = 0.1\lambda_0$. The electric field is calculated using the nearfield formulas in [23]. The SDFMM is compared with the sparse matrix canonical grid (SMCG) method [1] and excellent agreement is observed as shown in Figure 2. The incident angle is $\theta^i = 20°$, soil relative dielectric constant is $\varepsilon_r = 2.0 - i0.2$, and surface roughness parameters are rms height $\sigma = 0.02\lambda_0$ and correlation length $l_c = 0.5\lambda_0$. The comparison in Figure 2 shows the normalized radar cross section (RCS) for the HH-polarization case with horizontal axis to be the scatter angle θ (elevation angle in degrees) measured from the z-axis.

In this work, two types of soils have been studied: Bosnian soil with density 1.4 g/cm^3 and 3.8% moisture level with complex dielectric constant $\varepsilon_r = 3 - i0.18$ at 1 GHz [10], and Puerto Rican clay loam with density 1.2 g/cm^{3}and 10% moisture with dielectric constant $\varepsilon_r = 5.4 - i0.04$ at frequency $f =$ 960 MHz [11]. Three values of the rough ground rms height are assumed: $\sigma = 0.1\lambda_0$, $0.12\lambda_0$, and $0.17\lambda_0$ along with constant correlation length $l_c = 1\lambda_0$.

In Figures 3a–c, the mean scattered fields in air from Bosnian soil with different rms random heights are shown, while Figures 3d–f shows the transmitted fields. Note that for a perfectly flat ground surface, $\sigma = 0$; the contours would be perfect circles. In fact, with enough Monte Carlo runs, the mean scattered and transmitted field would be expected to be circularly symmetric for normal incidence. However, these mean fields show significant asymmetry and distortion, indicating that the random rough surface

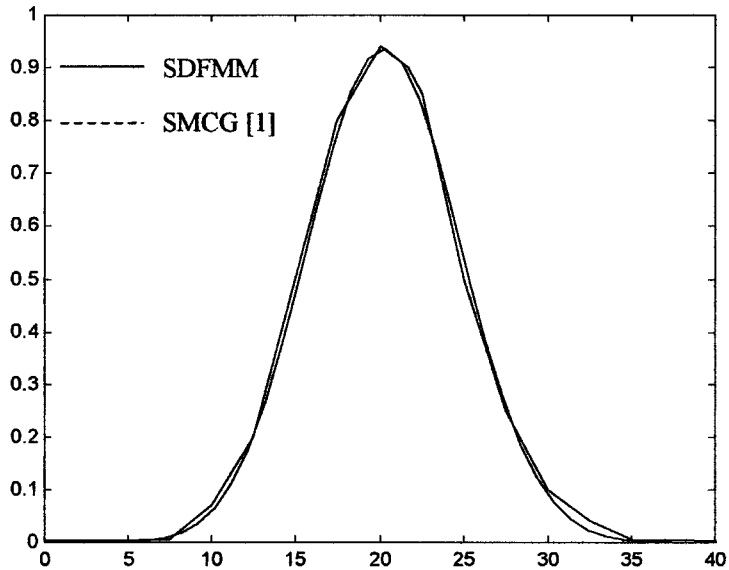

Figure 2. Normalized RCS for a rough surface of root mean square height $\sigma = 0.02\lambda_0$ and correlation length $l_c = 0.5\lambda_0$, at incident angle $\theta^i = 20°$. HH polarization.

causes so much variation in the scattered fields that 60 runs is insufficient for convergence. As the rms height of the rough surface increases, the distortion in both the mean scattered and transmitted field increases as well. The asymmetry of the mean scattered and transmitted wave patterns give a qualitative sense of the distorting effects of the rough surface. Moreover, the results show that the waves transmitted into the ground, Figures 3d–f, are less distorted than the scattered fields above the ground. This could be explained by noting that for rays incident on locally tilted surface patches (the sides of small hills and valleys), the reflected rays are bent further away from the nominal surface normal than the transmitted rays. As the surface roughness increases, the slopes of the surface patches increase, and the reflected rays diverge more. In Figures 4a–c and 4d–f, the scattered and transmitted fields from Puerto Rican soil with the same three rms random heights are shown. Comparing results of Figures 3 and 4, the magnitude of the scattered fields from the Puerto Rican soil is observed to be larger—and the transmitted fields smaller—than that of the Bosnian soil. This is consistent with the fact that the dielectric constant for Puerto Rican soil is almost double that of Bosnian soil. Greater distortion in the transmitted fields in the Puerto Rican soil is observed as compared with the Bosnian soil case

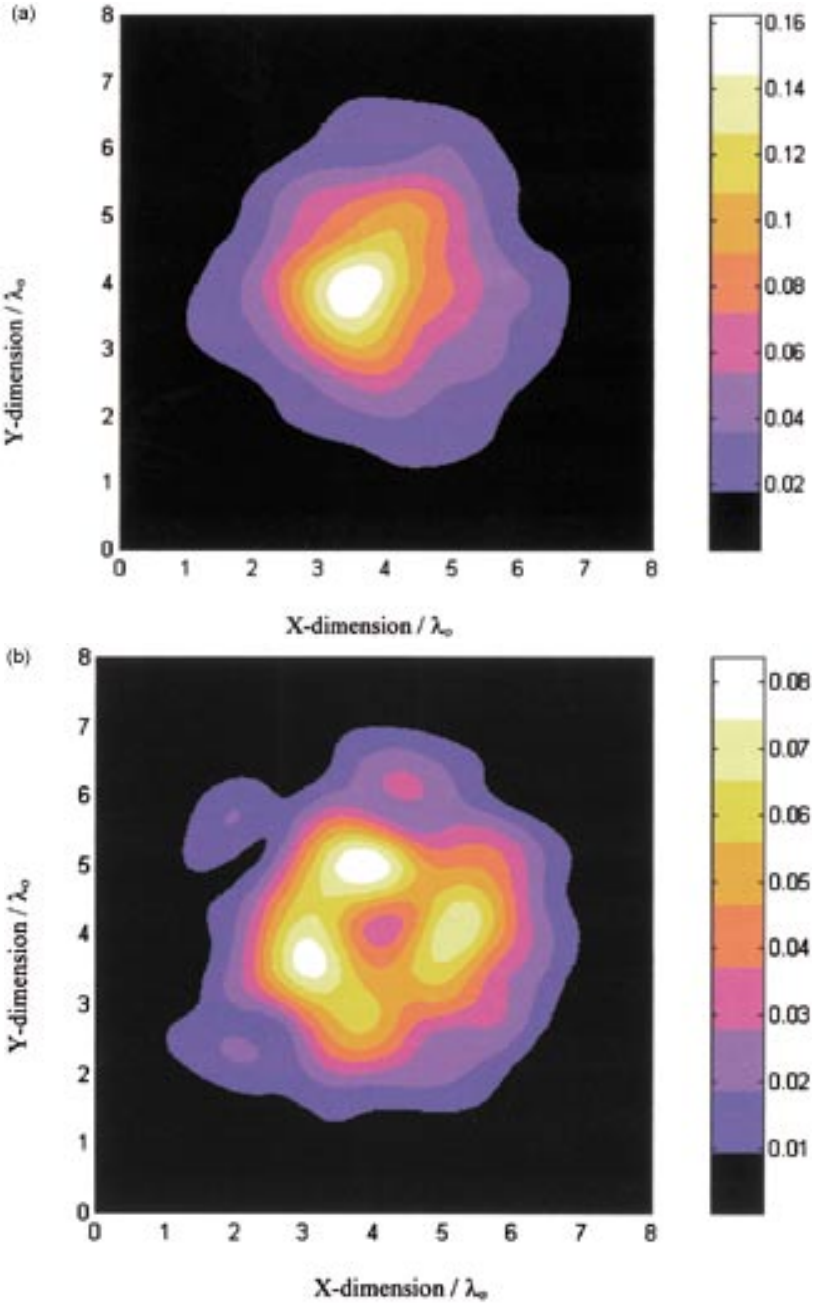

Figure 3. a) Near field scattered at $z = 1\lambda_0$ above the mean ground of Bosnian soil rough surface of root mean square height $\sigma = 0.1\lambda_0$ and correlation length $l_c = 1\lambda_0$, and incident angle $\theta^i = 0$. b) Near field scattered at $z = 1\lambda_0$ above the mean ground of Bosnian soil rough surface of root mean square height $\sigma = 0.12\lambda_0$ and correlation length $l_c = 1\lambda_0$, and incident angle $\theta^i = 0°$.

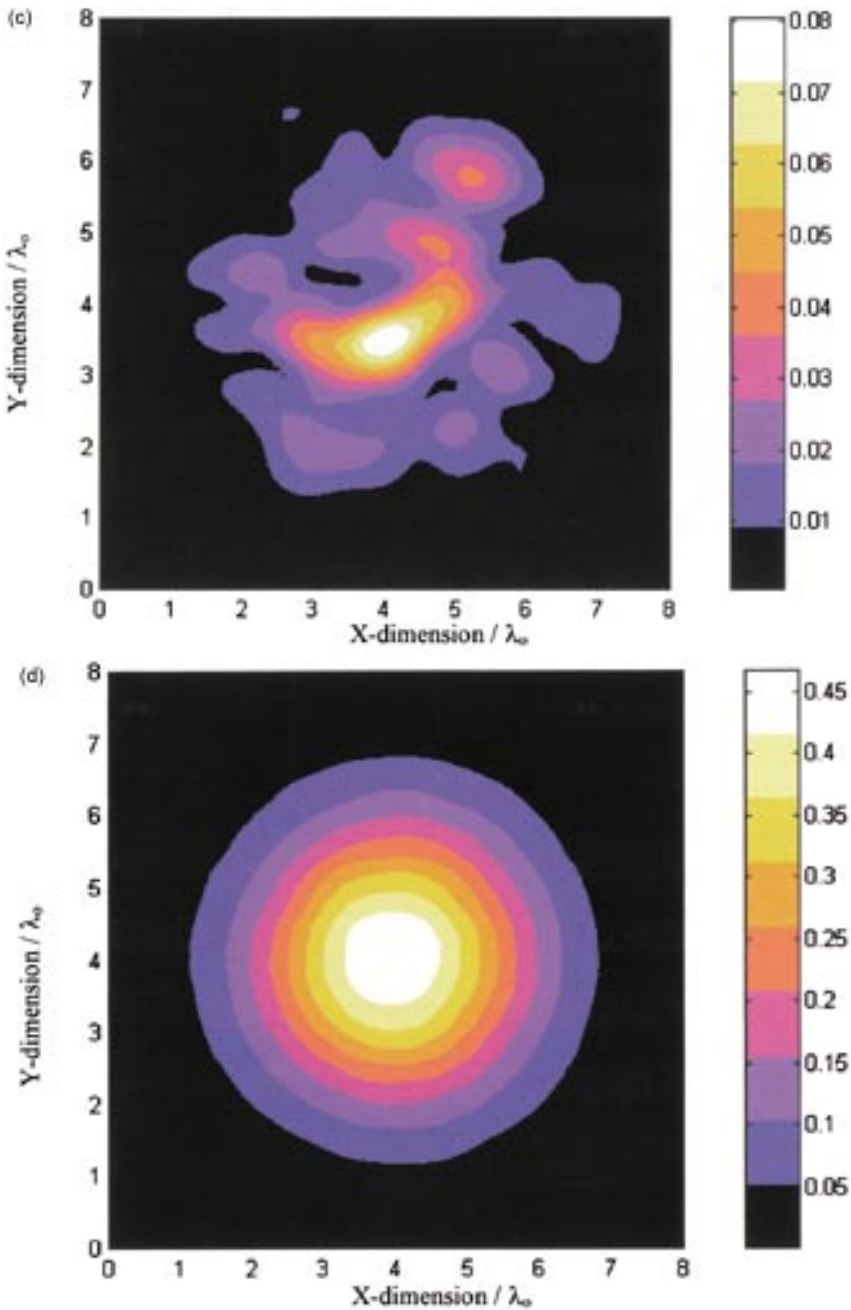

Figure 3 (continued). c) Near field scattered at $z = 1\lambda_0$ above the mean ground of Bosnian soil rough surface of root mean square height $\sigma = 0.17\lambda_0$ and correlation length $l_c = 1\lambda_0$, and incident angle $\theta^i = 0$. d) Near field transmitted at $z = -1\lambda_0$ below the mean ground of Bosnian soil rough surface of root mean square height $\sigma = 0.1\lambda_0$ and correlation length $l_c = 1\lambda_0$, and incident angle $\theta^i = 0$.

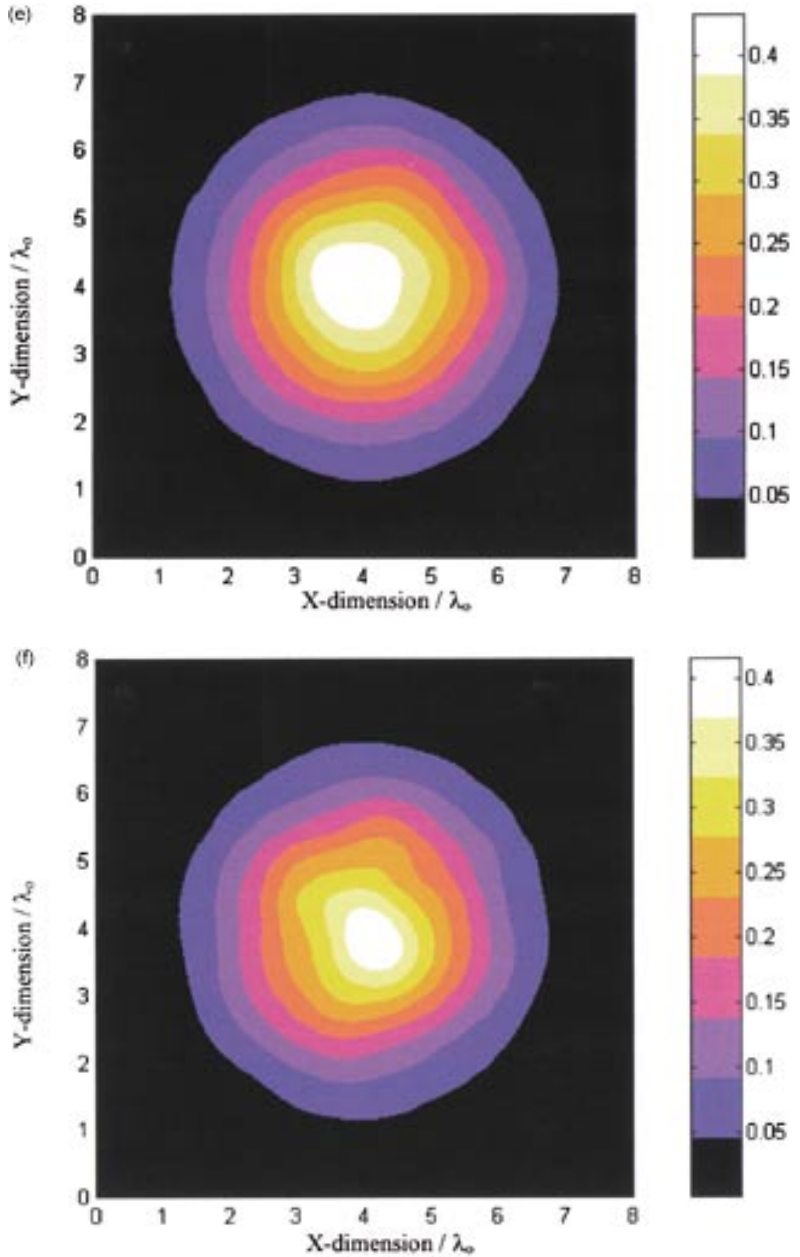

Figure 3 (continued). e) Near field transmitted at $z = -1\lambda_0$ below the mean ground of Bosnian soil rough surface of root mean square height $\sigma = 0.12\lambda_0$ and correlation length $l_c = 1\lambda_0$, and incident angle $\theta^i = 0$. f) Near field transmitted at $z = -1\lambda_0$ below the mean ground of Bosnian soil rough surface of root mean square height $\sigma = 0.17\lambda_0$ and correlation length $l_c = 1\lambda_0$, and incident angle $\theta^i = 0$.

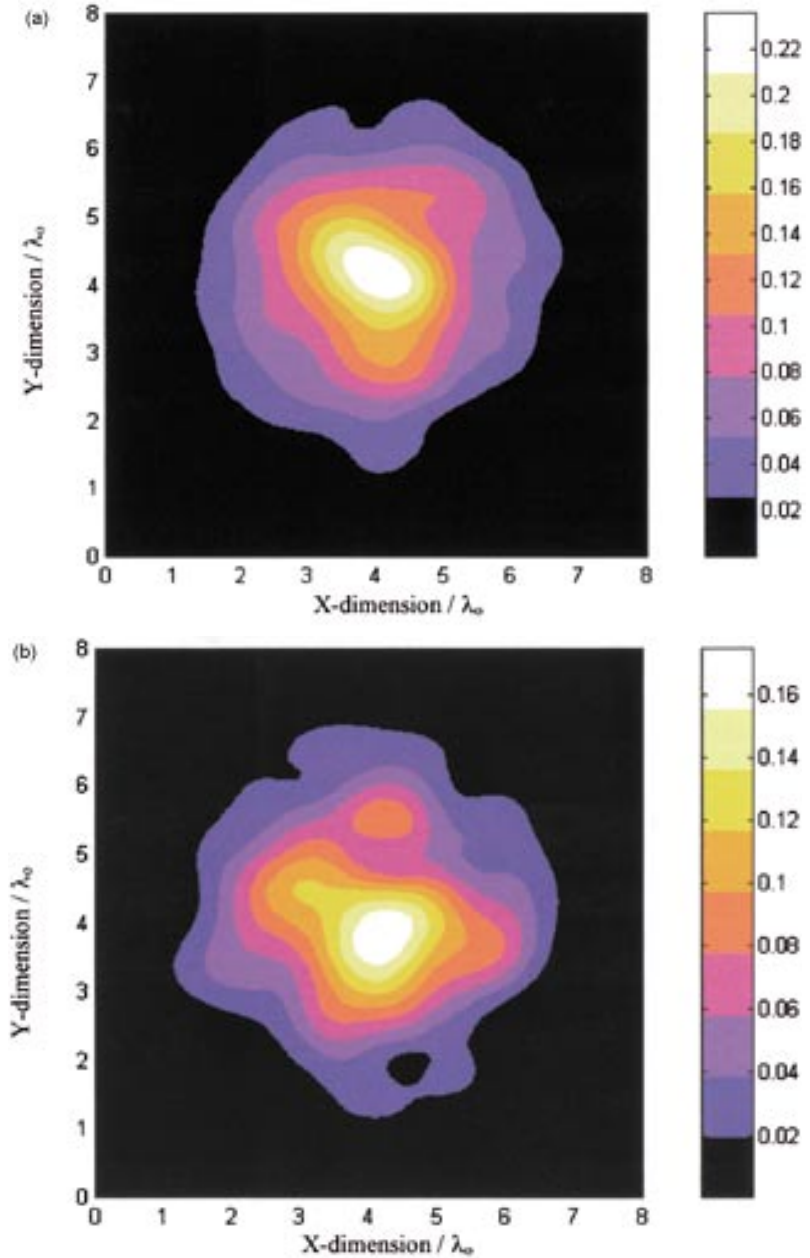

Figure 4. a) Near field scattered at $z = 1\lambda_0$ above the mean ground of Puerto Rican soil rough surface of root mean square height $\sigma = 0.1\lambda_0$ and correlation length $l_c = 1\lambda_0$, and incident angle $\theta^i = 0$. b) Near field scattered at $z = 1\lambda_0$ above the mean ground of Puerto Rican soil rough surface of root mean square height $\sigma = 0.12\lambda_0$ and correlation length $l_c = 1\lambda_0$, and incident angle $\theta^i = 0$.

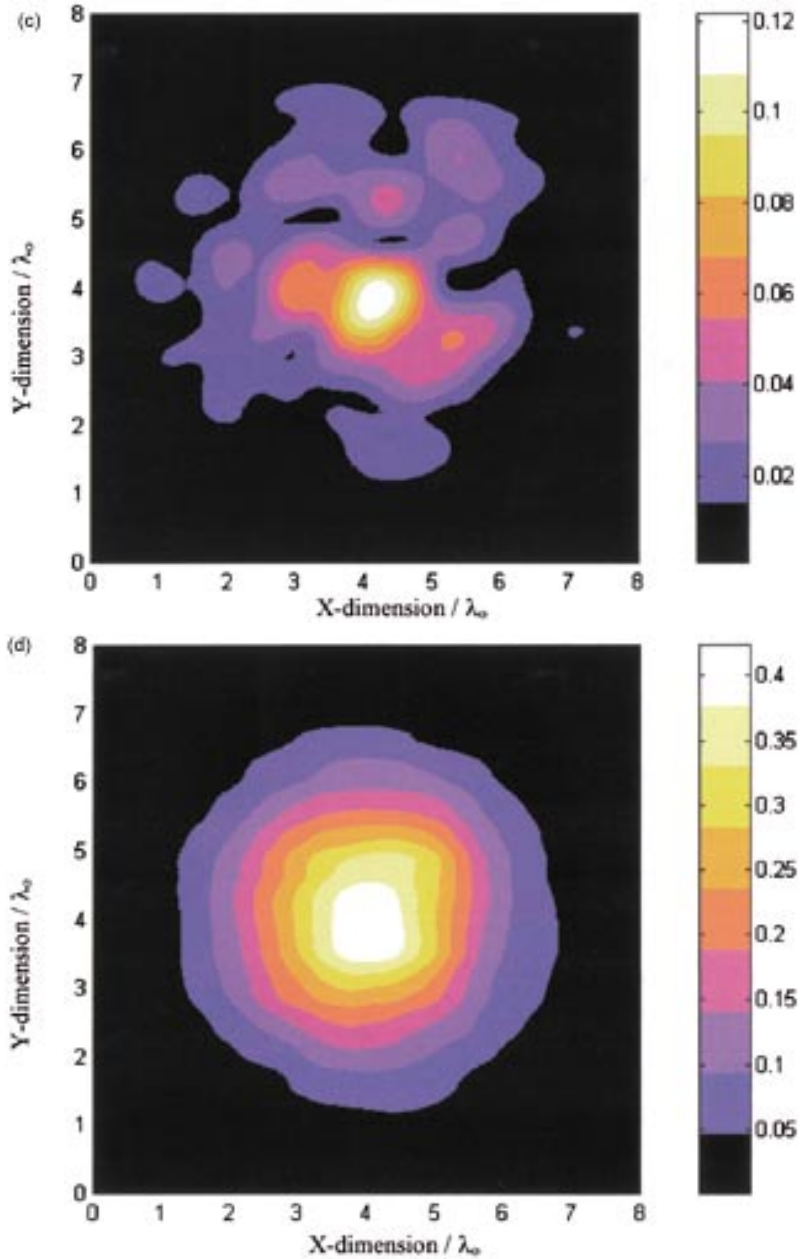

Figure 4 (continued). c) Near field scattered at $z = 1\lambda_0$ above the mean ground of Puerto Rican soil rough surface of root mean square height $\sigma = 0.17\lambda_0$ and correlation length $l_c = 1\lambda_0$, and incident angle $\theta^i = 0$. d) Near field transmitted at $z = -1\lambda_0$ below the mean ground of Puerto Rican soil rough surface of root mean square height $\sigma = 0.1\lambda_0$ and correlation length $l_c = 1\lambda_0$, and incident angle $\theta^i = 0$.

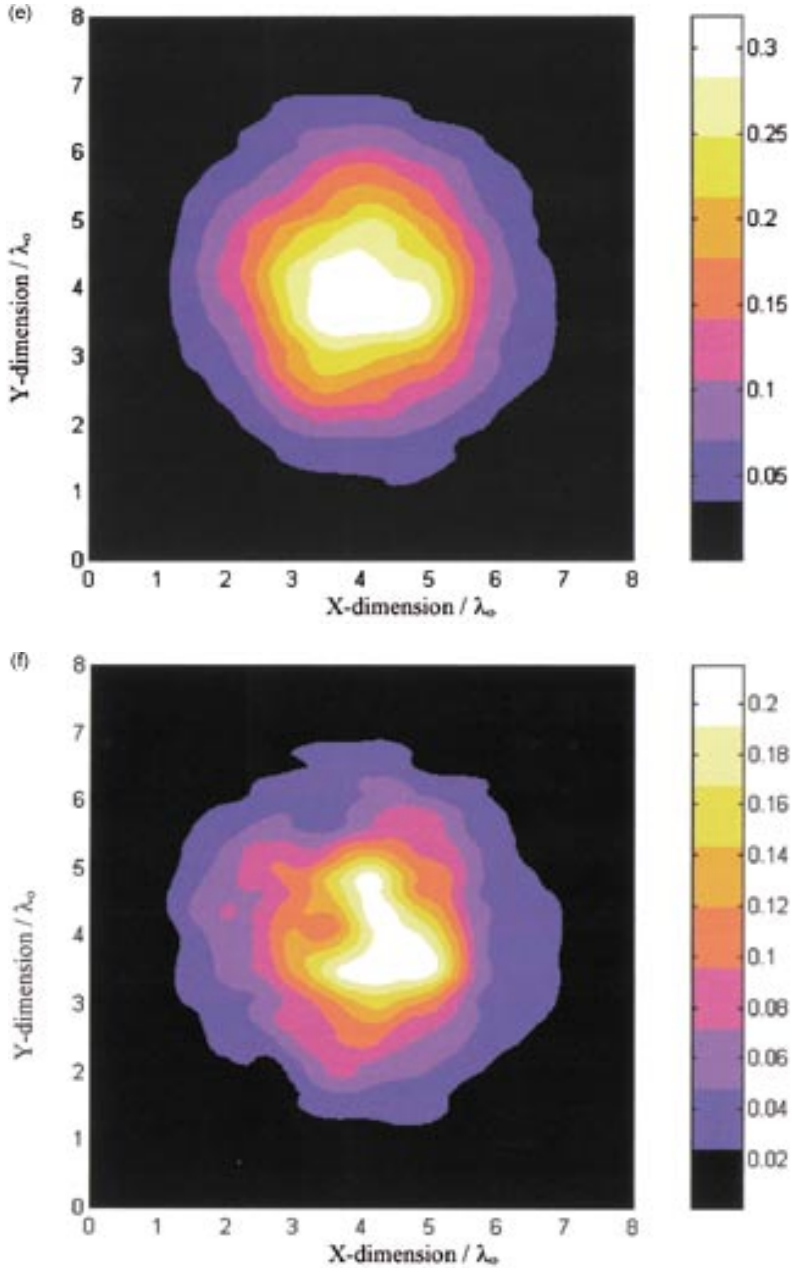

Figure 4 (continued). e) Near field transmitted at $z = -1\lambda_0$ below the mean ground of Puerto Rican soil rough surface of root mean square height $\sigma = 0.12\lambda_0$ and correlation length $l_c = 1\lambda_0$, and incident angle $\theta^i = 0$. f) Near field transmitted at $z = -1\lambda_0$ below the mean ground of Puerto Rican soil rough surface of root mean square height $\sigma = 0.17\lambda_0$ and correlation length $l_c = 1\lambda_0$, and incident angle $\theta^i = 0$.

(Figs. 4d–f vs. Figs. 3d–f). This results from the larger electrical distance in the former medium from the rough surface scattering centers to the observation plane one wavelength in air below the ground. The destructive interference of the transmitted Gaussian beam is enhanced when the phase differences from various parts of the surface proportionally increase.

Although the conductivity in soil plays an important role in subsurface sensing, it does not appear to have a dominant effect in the distortion of the transmitted Gaussian beam. A test of 60 Monte Carlo SDFMM runs of a fictitious soil medium with the real dielectric constant of Bosnian soil, but with the loss of the Puerto Rican clay loam indicates that the transmitted field has about the same distortion as for the actual Bosnian soil.

The total CPU time needed for filling the impedance matrix, for the iterative solution using the transpose free quasi-minimal residual solver (TFQMR) [24], and for calculating scattered and transmitted near fields is plotted vs. the rough surface rms height and shown in Figure 5. The discretization rate of the surface current, number of electric and magnetic surface current unknowns, and the required computer memory to run the SDFMM

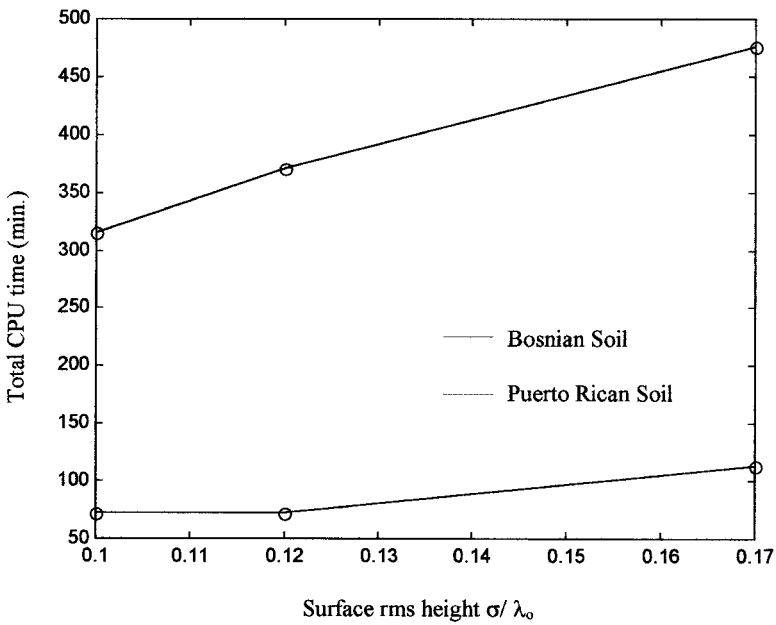

Figure 5. Total CPU time vs. the rms height of the rough surface.

Table 1.

	Bosnian soil	Puerto Rican soil
Discretization rate	$14/\lambda_0$	$18.5/\lambda_0$
Number of surface current unknowns	73,382	132,610
Required computer memory	800 MB	1.76 GB

code are given in Table 1. As expected, running the SDFMM code for the Puerto Rican soil required more CPU time and computer memory due to its larger relative dielectric constant requiring a finer discretization.

The NCSA SGI/CRAY Origin 2000 machines are used for the Puerto Rican case due to its larger memory requirement, but the Compaq GS140 EV6 machine at Northeastern University is used for the Bosnian case, which reflects the results shown in Figure 5.

4. Conclusions

The SDFMM fast algorithm is used to calculate the nearfield scattered from and transmitted into two types of rough ground soils. Bosnian and Puerto Rican soils were chosen for this study as *a priori* phase of our investigation of scattering from buried mines under the same types of soils [22]. The results show that the distortion in both the scattered and the transmitted fields increases as the ground roughness increases. We observed that the scattered fields experience more distortion than the transmitted ones. This suggests a future research to investigate how the transmitted fields will be changing with the increase of the incident angle. This result indicates that although rough surfaces randomly distort both the scattered and transmitted waves, the distortion is greater for the former. Thus the uncertainty of the surface clutter signal is greater than that of the probing signal, suggesting the relative importance of careful characterization of the scattered waves.

Acknowledgments

The authors would like to thank Prof. W. Chew, Prof. E. Michielssen, and Dr. V. Jandhyala at UIUC for allowing us to use and modify the SDFMM computer code for the current application. This research was sponsored by the Army Research Office Demining MURI grant no. DAA 0-55-97-0013 and in part by the Engineering Research Centers Program of the NSF under award number EEC-9986821. The computational work was partially supported by National Computational Science Alliance under grant no. pt1 and utilized the NCSA SGI/CRAY Origin 2000 and the

allocation of time at the Northeastern University Advanced Scientific Computation Center (NU-ASCC).

References

1. Zhang, G., Tsang, L., and Pak, K., 1998, Angular correlation function and scattering coefficient of electromagnetic waves scattered by a buried object under a two-dimensional rough surface: J. Opt. Soc. Am. A., p. 2995–3002.
2. Zhang, Y. and Bahar, E., 1999, Müeller matrix elements that characterize scattering from coated random rough surfaces: IEEE Trans. on Antenn. and Propag., v. 47, no. 5, p. 949–955.
3. Ishimaru, A. and Chen, J.S., 1991, Scattering from very rough metallic and dielectric surfaces: a theory based on the modified Kirchhoff approximation: Waves in Random Media, p. 21–34.
4. Mainguy, S. and Greffet, J., 1998, A numerical evaluation of Raleigh's theory applied to scattering by randomly rough dielectric surfaces: Waves in Random Media, p. 79–101.
5. Kapp, D.A. and Brown, G.S., 1996, A new numerical method for rough surface scattering calculations: IEEE Trans. on Antenn. and Propag., v. 44, no. 5, p. 711–721.
6. Fung, A.K., Shah, M.R., and Tjuatja, S., 1994, Numerical simulations of scattering from three-dimensional randomly rough surfaces: IEEE Trans. Geoscience Rem. Sensing, v. 32, no. 5, p. 986–994.
7. Nieto-Vesperinas, M. and Sa′nchez-Gil, J.A., 1993, Intensity angular correlations of light multiply scattered from random rough surfaces: J. Opt. Soc. Am. A, v. 10, no. 1, p. 150–157.
8. Johnson, J.T., 1999, Third order small perturbation method for scattering from dielectric rough surfaces: J. Opt. Soc. Am. A, v. 16, no. 11, p. 2720–2736.
9. Xiong, Z. and Tripp, A.C., 1997, 3-D electromagnetic modeling for near-surface targets using integral equations: Geophysics, v. 62, no. 4, p. 1097–1106.
10. Curtis, J., 1996, Dielectric properties of soils; various sites in Bosnia: US Army Corp. of Eng., Waterways Experim. Station Data Rep.
11. Hipp, J.E., 1974, Soil electromagnetic parameters as functions of frequency: soil density and soil moisture: Proceedings of the IEEE, v. 62, no. 1, p. 98–103.
12. Garcia, N. and Stoll, E., 1984, Monte Carlo calculation for electromagnetic-wave scattering from random rough surfaces: Phy. Rev. Let., v. 52, no. 20, p. 1798–1801.
13. Rokhlin, V., 1990, Rapid solution of integral equations of scattering theory in two dimensions: J. Comput. Phys., 36, p. 414–439.
14. Lu, C.C. and Chew, W.C., 1993, Fast algorithm for solving hybrid integral equations: IEE Proceedings-H, v. 140, no. 6.
15. Jandhyala, V., 1998, Fast multilevel algorithms for the efficient electromagnetic analysis of quasi-planar structures: PhD thesis, Department of Electrical Engineering, University of Illinois at Urbana-Champaign, 1998.
16. Jandhyala, V., Shanker, B., Michielssen, E., and Chew, W.C., 1998, A fast algorithm for the analysis of scattering by dielectric rough surfaces: J. Opt. Soc. Am. A, v. 15, no. 7, p. 1877–1885.
17. El-Shenawee, M., Jandhyala, E., Michielssen, E., and Chew, W.C., 1998, An enhanced steepest descent fast multipole method for the analysis of scattering from two dimensional multilayered rough surfaces: Proceedings of the URSI '98 conference, Atlanta, p. 182.
18. El-Shenawee, M., Jandhyala, E., Michielssen, E., and Chew, W.C., 1999, The steepest descent fast multipole method (SDFMM) for solving combined field integral equation pertinent to rough surface scattering: Proceedings of the IEEE APS'99, Orlando.

19. Medgyesi-Mitschang, L., Putnam, J., and Gedera, M., 1994, Generalized method of moments for three-dimensional penetrable scatterers: J. Opt. Soc. Am. A, v. 11, no. 4, p. 1383–1398.
20. Rao, S.M., Wilton, D.R., and Glisson, A.W., 1982, Electromagnetic scattering by surfaces of arbitrary shape: IEEE Trans. on Anten. and Prop., v. AP 30, no. 3, p. 409–418.
21. Tran, P. and Maradudin, A.A., 1992, Scattering of a scalar beam from a two-dimensional randomly rough hard wall: enhanced backscatter: Phy. Rev. B, v. 45, no. 7, p. 3936–3939.
22. El-Shenawee, M., Rappaport, C., Miller, E., and Silevitch, M., 2001, 3-D subsurface analysis of electromagnetic scattering from penetrable/PEC objects buried under rough surfaces: use of the steepest descent fast multipole method (SDFMM): to be published in the IEEE Trans. Geoscience Rem. Sensing.
23. Balanis, C.A., 1989, Advanced Engineering Electromagnetics, John Wiley & Sons Inc, ch. 6, p. 254–309.
24. Freund, R.W., 1993, A transpose-free quasi-minimal residual algorithm for non-Hermitian linear systems: SIAM J. Sci. Comput., v. 14, no. 2, p. 470–482.